

Failure of t - J models in describing doping evolution of spectral weight in x-ray scattering, optical, and photoemission spectra of cuprates

R. S. Markiewicz, Tanmoy Das, and A. Bansil

Physics Department, Northeastern University, Boston, Massachusetts 02115, USA

(Received 8 June 2010; published 1 December 2010)

We have analyzed experimental evidence for an anomalous transfer of spectral weight from high- to low-energy scales in both electron- and hole-doped cuprates as a function of doping. X-ray scattering, optical, and photoemission spectra are all found to show that the high-energy spectral weight decreases with increasing doping at a rate much faster than predictions of the large U -limit calculations. The observed doping evolution is however well described by an intermediate coupling scenario where the effective Hubbard U is comparable to the bandwidth. The experimental spectra across various spectroscopies are inconsistent with fixed- U exact diagonalization or quantum Monte Carlo calculations, and suggest a significant doping dependence of the effective U in the cuprates.

DOI: [10.1103/PhysRevB.82.224501](https://doi.org/10.1103/PhysRevB.82.224501)

PACS number(s): 71.10.-w, 71.30.+h, 71.35.-y, 71.45.-d

I. INTRODUCTION

The key to unraveling the mechanism of cuprate superconductivity is to ascertain the effective strength of correlations since pairing is widely believed to arise from electron-electron interactions rather than from the traditional electron-phonon coupling. Two sharply different scenarios have been proposed and remain subject of considerable debate. One viewpoint holds that $U \gg W$, where U is the Hubbard U and $W \sim 8t$ is the bandwidth with hopping parameter t . In this case, a “pairing glue” is not necessary as the pairs are bound by a superexchange interaction $J=4t^2/U$, and the dynamics of the pairs involves virtual excitations above the Mott gap set by the energy scale U .¹ In the opposing view, $U \sim W$, and pairing is mediated by a bosonic “glue,” which originates from antiferromagnetic (AFM) spin fluctuations.^{2,3} It is clear thus that the determination of the size of the effective U and its variation with doping are essential ingredients for understanding the mechanism of superconductivity as well as the magnetic phase diagram of the cuprates.

Since the electronic dispersion at half filling has a gap of magnitude $\sim U$ which is clearly visible in x-ray absorption (XAS), angle-resolved photoemission (ARPES), and optical spectra, one way to estimate the size of U is to follow the evolution of high-energy spectral weight as a function of doping. Whereas for a conventional band insulator the spectral weights of the bands above and below the gap are independent of doping, this is not the case for a Mott insulator. In the latter case, for $U \rightarrow \infty$, removing one electron creates *two* low-energy holes—one from the lower Hubbard band (LHB), but a second one from the upper Hubbard band (UHB), since without an electron on the atom there is no U penalty in adding an electron. Paradoxically, as U decreases, the rate of this anomalous spectral weight transfer (ASWT) actually increases.⁴⁻⁶ For infinite U double occupancy (DO) is always forbidden, so no matter how few electrons are in the LHB, there will be an equivalent number of holes in the UHB. In contrast, for smaller U values DO is reduced collectively via long-range magnetic order. As the magnetic order disappears at a quantum critical point,^{7,8} a much higher degree of DO is restored, and the UHB can completely vanish.

Hence, by measuring the high-energy spectral weight (HESW) as a function of doping, we can estimate the degree of correlation in cuprates. Here we quantify these results for XAS, ARPES, and optical measurements, and demonstrate that the doping evolution of ASWT is similar across all these spectroscopies for both electron- and hole-doped cuprates. Moreover, the observed doping evolution is inconsistent with large U values, and also with fixed- U Hubbard model calculations but it is consistent with a doping-dependent effective U of intermediate strength $U \lesssim W$.

This paper is organized as follows: in Sec. II we explain how to quantify the rate of ASWT with doping, and show that similar rates are found for several different spectroscopies. In Sec. III we show that these rates are consistent with an intermediate coupling model of the cuprates. A discussion of the results is given in Sec. IV, and conclusions are presented in Sec. V.

II. QUANTIFYING ANOMALOUS SPECTRAL WEIGHT TRANSFER

We motivate a definition of the rate of ASWT with doping in Fig. 1(a). In a strongly correlated system, removing x electrons from the undoped system leaves $(1+x)$ empty states above the Fermi level, which are distributed between $p \geq 2x$ low-energy (in-gap) states and $W_{\text{UHB}}=1+x-p$ states in the UHB. Then the ASWT can be quantified by the coefficient β , defined such that in this process the weight of the UHB reduces to $W_{\text{UHB}}=1-\beta x$ and the low-energy holes gain weight by $p=(1+\beta)x$. The value of β is found theoretically to depend on U such that $\beta=1$ for a very strongly correlated ($U \rightarrow \infty$) Mott insulator while reducing U leads to larger values of β . Figure 1(b) illustrates a variety of calculations of the HESW vs doping. Exact diagonalization (ED) calculations on small clusters^{4,9} (dashed lines) find $\beta=1$ for the t - J model or for a $U \rightarrow \infty$ Hubbard model, $\beta \approx 1.5$ (at low doping) for $U=10t$, and $\beta \approx 2.0$ for $U=5t$. Shown also in Fig. 1(b) are quantum Monte Carlo (QMC) results for $U=8t$, $t'=0$ (where t and t' are hopping parameters),^{10,11} which are consistent with the ED results. Hence, $\beta=1$ confirms strong correlations and the “no double occupancy” hypoth-

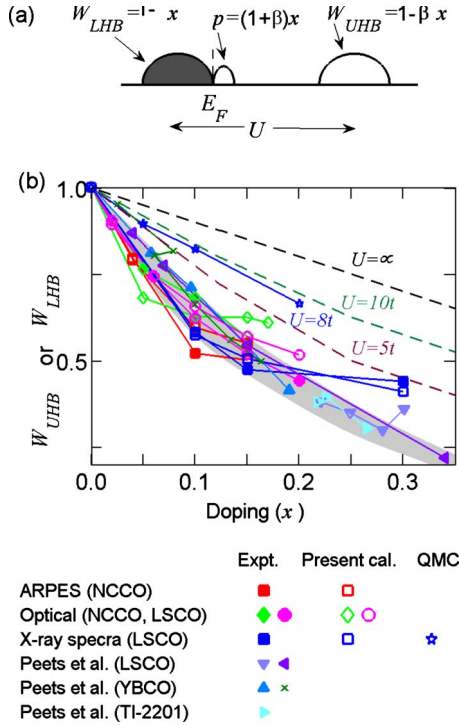


FIG. 1. (Color online) (a) Schematic of ASWT for hole-doped cuprates. (b) Estimates of W_{UHB} (for hole doping) and W_{LHB} (for electron doping) from various experimental results (see legend) (Refs. 12–17) are compared with our theoretical results (open symbols of same color). Dashed lines of various colors show exact diagonalization calculations for different values of U taken from Ref. 4. QMC results (Refs. 10 and 11) from Fig. 4 are plotted as blue stars. All curves are normalized to $W_{UHB} \rightarrow 1$ at half filling.

esis while a faster falloff ($\beta > 1$) indicates otherwise, and supports a real gap collapse model ($W_{UHB} \sim 0$ at $x = 1/\beta$). For an electron-doped system the HESW is associated with the LHB, and is described by the mirror image of Fig. 1(a) with respect to E_F .

Shown also in Fig. 1(b) is our key result, the HESW of a variety of cuprates as a function of doping, extracted from a number of spectroscopies. The results are strikingly similar over a variety of spectroscopies, as expected but also over several families of cuprates for both electron and hole doping. Shown in Fig. 1(b) are XAS results on $\text{La}_{2-x}\text{Sr}_x\text{CuO}_4$ (LSCO),¹² ARPES on $\text{Nd}_{2-x}\text{Ce}_x\text{CuO}_{4\pm\delta}$ (NCCO),¹³ and optical absorption on both NCCO (Refs. 14 and 15) and LSCO,¹⁶ compared with additional XAS data for LSCO, $\text{YBa}_2\text{Cu}_3\text{O}_{6+x}$, and $\text{Ti}_2\text{Ba}_2\text{CuO}_6$ from Ref. 17. All experimental measures of HESW find a rapid falloff of the spectral weight with doping, and at low doping decrease almost linearly with doping with approximately the same slope of $\beta \approx 3.7$, consistent with $U_{eff} < 5t$, suggesting that the cuprates are far from the strong correlation limit. The observed falloff supports a real gap collapse at $x_{UHB} \sim 1/\beta = 0.27$. Notably, the value of U_{eff} is incompatible with the measured gap at half filling. For example, optical spectra find a gap consistent with $U \sim 8t$, but the HESW calculations for fixed $U = 8t$ are far from the experimental results. On the other hand, the experimental data can be explained by intermediate coupling

model calculations^{18–20} with a doping-dependent effective U . The calculated results are plotted in Fig. 1(b) as open symbols of same color as the corresponding experimental data.

Since the HESW is an intrinsic property of the electronic structure of cuprates, it should show up in all spectral probes, and Fig. 1(b) confirms this. However, it is important to realize that the ASWT will play out quite differently in different spectroscopies. First, as is clear from Fig. 1(a), there is a strong electron-hole asymmetry to the effect: the changes will be much smaller in the Hubbard band which lies at the Fermi level. Hence, for maximum sensitivity to ASWT in a hole-doped cuprate, the probe should be sensitive to empty states, and to filled states for electron-doped cuprates. Thus, ARPES (Ref. 21) or x-ray emission spectroscopies are well suited for studying ASWT in electron-doped cuprates while XAS is appropriate for hole-doped cuprates. Optical¹⁸ and resonant inelastic x-ray scattering^{22,23} studies would work for both cases, as they measure a joint density of states (DOS). On the other hand, Compton scattering²⁴ and positron annihilation²⁵ will not be sensitive to ASWT because these spectroscopies measure only the total spectral weight of occupied states but not how this spectral weight gets rearranged in energy with doping. In principle, scanning tunneling microscopy²⁶ could follow either sign of charge but would require a wide energy range, ~ 2 eV to see the full effect.

Figure 2 illustrates how the experimental ASWTs of Fig. 1(b) were extracted. The ARPES, optical, and XAS data are shown as dashed lines in the upper panel of Fig. 2, and the corresponding integral, representing the electron number $n(\omega)$, in the lower panel of Fig. 2. In each spectrum, the UHB (LHB for electron doping) is denoted by a gray shaded region, and the W_{UHB} (or W_{LHB}), Fig. 1(b), is defined as the integrated density over that region, starting from a cut-off frequency ω_c , taken as independent of doping. A complication is involved in comparing our one-band calculation with the experimental data, in that the antibonding band in cuprates lies near to other bands, and the role of the latter must be disentangled before the spectral weight can be estimated. At high energies, we subtract off a background from the experimental spectra associated with interband transitions to higher-lying bands not included in the present one-band calculations.^{18,27–30} We use a doping-independent background contribution shown as black dashed lines in Figs. 1(a)–1(d). In all cases we compare the data with calculations based on the quasiparticle-GW (QP-GW) model^{18,31} (solid lines), discussed below.

For electron doping, ARPES can detect the full LHB and hence determine W_{LHB} to the extent that matrix element effects are doping independent.²⁰ The ARPES results for NCCO are compared with our theoretical results in Fig. 2(a). At half filling the energy distribution curve along the nodal direction shows the so-called charge-transfer gap from the Fermi level to the LHB. A significant redistribution of spectral weight is evident at $x = 0.04$ as the LHB approaches the Fermi level and by $x = 0.10$, virtually all of the spectral weight of the LHB has shifted to the vicinity of the Fermi level. The top of the LHB crosses E_F at $x \approx 0.15$, forming a hole pocket, and the spectral weight near E_F undergoes an abrupt increment. To extract the total spectral weight associated with the LHB we have integrated the spectral weight

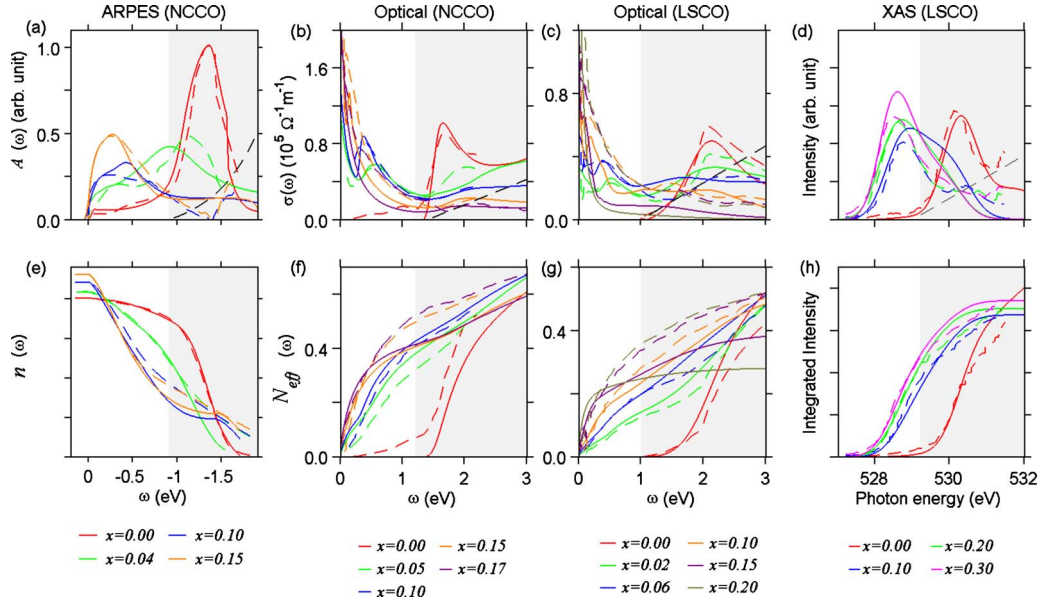


FIG. 2. (Color online) (a) ARPES spectra along the nodal direction of NCCO for various dopings (Ref. 13). (b) and (c) Optical conductivity of NCCO (Ref. 14) and LSCO (Ref. 16). (d) K -edge XAS results (Refs. 12 and 17) are compared with our theoretical DOS (broadened with experimental resolution of 0.4 eV and shifted by a doping independent x-ray edge energy value of 528.4 eV). All spectra are subtracted from a doping-independent background associated with higher-energy bands (Ref. 27) shown as black dashed lines in frames (a)–(d). (e)–(h) Integrated spectral weights corresponding to the background subtracted spectra in the corresponding upper panels. (e) Integrated ARPES spectral weight (integrated around a small momentum window to mimic the experiment and averaged over nodal and antinodal directions), normalized to $(1+x)$ at E_F . (f) and (g) Effective number of electrons [Eq. (1)] calculated from the optical spectra for NCCO and LSCO. (h) Integrated XAS intensity. In all frames, dashed lines are experimental data (Refs. 13 and 14); solid lines of same color are the present calculations while the edge of the shaded region marks the crossover energy ω_c , discussed in the text.

from -1.9 eV to ω , Fig. 2(e). ARPES data are available along only two high-symmetry directions, so we take their average as representative of the net spectral weight, and at each doping normalize $n(\omega)$ to $(1+x)$ at E_F .

In Figs. 2(b) and 2(f), analysis of the HESW in NCCO based on the optical absorption spectra^{15,16} proceeds similarly.¹⁸ There is a large Mott gap below 2 eV in the undoped material but with doping there is a strong transfer of spectral weight from the gap to low-energy features—the Drude peak and the midinfrared (MIR) peak—with an isosbestic (equal absorption) point around $\omega \sim 1.3$ eV. As a measure of the HESW, the effective electron number (per Cu atom) is obtained as

$$N_{eff}(\omega) = \frac{2m_0V}{\pi e^2 \hbar} \int_{-\infty}^{\omega} \sigma(\omega') d\omega', \quad (1)$$

where m_0 and e are the free-electron mass and charge and V is the volume of a unit cell. The weight of the LHB is extracted as $W_{LHB} = 1+x - N_{eff}(\omega_c)$. A similar analysis of W_{UHB} was carried out on LSCO spectra¹⁶ in Figs. 2(c) and 2(g), and the results are included in Fig. 1(b). These optical results are consistent with the analysis of Comanac *et al.*²⁹ It is interesting to note that the ω_c which separates the high-energy Hubbard bands and the low-energy in-gap states coincides with the isosbestic or equal absorption point in the optical spectra, i.e., the residual charge-transfer gap.

For hole doping, W_{UHB} was determined by XAS,^{12,17} which detects the empty states above the E_F . In this spirit, we

compare the measured XAS spectra with the calculated empty-state DOS in Figs. 2(d) and 2(h). The behavior of the spectral weight transfer is very similar to the ARPES result for NCCO in Fig. 2(a).

The overall similarity of the doping dependence of the excess electron (or hole) count $n(\omega)$ between ARPES, optical and XAS experiments is striking, and is well captured in the model calculations in Figs. 2(e)–2(h). The HESW plotted in Fig. 1(b) illustrates one important characteristic of these curves to demonstrate the universality of the doping dependence but the detailed agreement is clearly much more extensive. This observation motivates our choice of the cut-off frequencies in Fig. 2. Since experimental and theoretical values are extracted in the same way, it is simplest to choose a doping-independent ω_c for each spectroscopy. The natural choice is the minimum spectral weight regions evident in Fig. 2, separating low- and high-energy scales. These correspond to the waterfall region in single-particle spectra of ARPES and XAS or the isosbestic point in optical spectra which is also the manifestation of the waterfall effect as discussed in Ref. 18. Our ω_c values are chosen as average values which fall near this minimum.

III. INTERMEDIATE COUPLING MODEL OF ASWT

The theoretical calculations in Figs. 1 and 2 are based on the QP-GW model,^{18,31} an extension of our earlier Hartree-Fock model of AFM gap collapse^{7,8,32,33} to the intermediate coupling regime by introducing a GW-like self-energy correction.^{34–37}

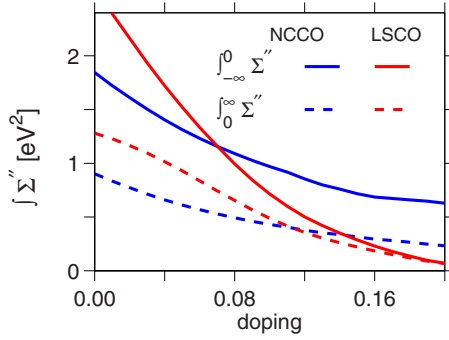


FIG. 3. (Color online) Integrated imaginary part of the calculated self-energy as a function of doping.

The self-energy Σ in QP-GW model is dominated by a broad peak in its imaginary part Σ'' which produces the “waterfall” effect^{19,20} in the electronic dispersion by redistributing spectral weight into the coherent in-gap states and an incoherent residue of the undressed UHB and LHB. With underdoping, the in-gap states develop a pseudogap which we model as a (π, π) -ordered spin-density wave. The doping evolution of both electron- and hole-doped cuprates is dominated by a magnetic gap collapse near optimal doping.^{7,8} The present calculations are obtained with the same parameter sets as in Ref. 18; in particular, the doping dependence of U is shown in Fig. 5 of that publication. Our analysis identifies two main factors that cause ASWT. First, the pseudogap collapses with doping, shifting the optical MIR peak to low energies while transferring weight to the Drude peak. Second, the residual incoherent weight associated with the Hubbard bands decreases with doping¹⁸ due to decrease in magnon scattering. This is reflected in the doping dependence of the peak in Σ'' . The strength of this peak can be measured by the area under the Σ'' curve, Fig. 3. This gives a direct measure of the tendency of the spectrum to split into coherent and incoherent parts, and hence a measure of the weight of the Hubbard bands. Figure 3 shows this quantity as a function of doping above and below the Fermi level for both NCCO and LSCO. In both materials, $\int \Sigma'' d\omega$ below E_F , seen in ARPES, shows a much faster falloff with doping. This fast falloff seems to terminate around $x \sim 0.20$ – 0.25 close to the point where the HESW extrapolates to zero, $x_{\text{UHB}} = 1/\beta \sim 0.25$. This is also close to the doping where AFM order ends in a critical point, suggesting an intimate connection between the decrease in magnon scattering and the collapse of the AFM gap. The good agreement between experiment and theory suggest that ASWT is predominantly associated with electron-electron interaction.³⁸

The unusual doping dependence of the experimental W_{UHB} in Fig. 1(b) can be understood within our model as follows. The magnetic gap collapses near $x \sim 0.2$ for both electron-^{32,33} and hole-doped case,⁸ and beyond this doping there is at most only a weak dip in the density of states, indicating a separation of the band into two components—now coherent and incoherent parts. However, since we work with fixed cutoff, we count all empty states in the band above ω_c as part of the UHB. These change slowly with doping, decreasing linearly to zero at $x=1.0$. Hence the break in slope indicates the magnetic gap collapse.

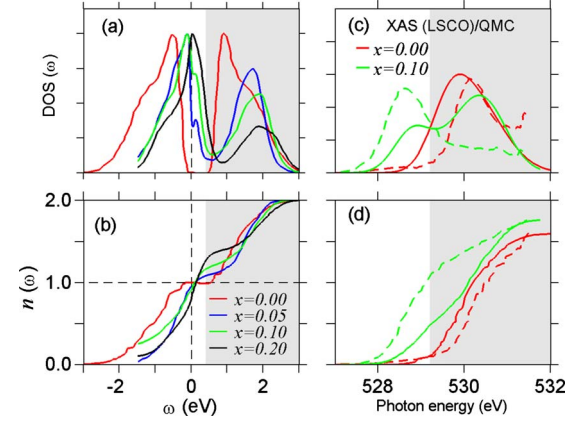


FIG. 4. (Color online) (a) DOS computed in QMC (Refs. 10 and 11). All results are normalized to their peak values. (b) Corresponding electron number $n(\omega)$, the integral of the DOS, normalized to 2 for a full band. The QMC results for some of the dopings are not available at higher energies below E_F , so we normalize $n(\omega)$ to $(1-x)$ at E_F . (c) and (d) QMC DOS with experimental broadening and K -edge energy shift (solid lines) is compared with experimental data (dashed lines) (Refs. 12 and 17) as in Figs. 2(d)–2(h).

IV. DISCUSSION

To better understand the failure of QMC calculations with fixed $U=8t$ to explain the observed ASWT, in Figs. 4(a) and 4(b) we plot the DOS and the associated electron count calculated in QMC.^{10,11} For $\omega_c=0.4$ eV, close to the DOS minimum,³⁹ W_{UHB} is in good agreement with the exact diagonalization results for the corresponding $U=8t$,⁴⁰ blue stars in Fig. 1(b) but has a considerably weaker falloff than found in experiment. Note that the same result would follow by choosing a doping dependent ω_c pinned to the DOS minimum. Consistent with this, we carried out a similar analysis of the XAS spectra based on QMC-based DOS with doping-independent $U=8t$ in Figs. 4(c) and 4(d). The QMC spectra (solid lines) are not consistent with the experimental results, clearly overestimating the weight of the UHB for finite dopings. Similar conclusions were reached in Refs. 17 and 41. Note that the mean-field result is similar: for $U=8t$, the gap collapse would be shifted to much higher doping $x \sim 0.43$.³²

Notably, the doping dependence of U could, in principle, be associated with correlation effects within a one-band Hubbard model, which are not accounted for in the present calculations. However, on this issue the theoretical situation is unsettled: neither exact diagonalization nor QMC with $U=8t$ captures the ASWT as shown in Fig. 1(b). On the other hand, recent DMFT calculations have been found to correctly describe the doping evolution of the cuprates with fixed- U models.^{29,41,42} One possible explanation for this difference is that the former calculations are for a pure Hubbard model while the DMFT calculations include next-nearest-neighbor hopping. Interestingly, we have found that the doping dependence of U can be explained by long-range Coulomb screening,¹⁸ and that this doping dependence is also reduced significantly in going to a three-band model.^{22,43} But multiple band and long-range Coulomb effects are not included in the Hubbard model, and will therefore not be cap-

tured in the QMC, exact diagonalization or DMFT calculations alluded to above.

V. CONCLUSIONS

In conclusion, we have shown that the spectral weight of the UHB (LHB for electron-doped cuprates) collapses with doping at a rate much faster than can be explained in a t - J or $U=\infty$ Hubbard model. Such a fast falloff would seem to require a real Mott gap collapse consistent with an intermediate coupling $U < W$ scenario. We find that the rate of ASWT is universal—the same across several spectroscopies and many different cuprates. The plot of HESW vs doping in Fig. 1(b) provides a unique signature of the effective Hubbard U in these materials.

Note added in proof. Reference 44 shows that introducing a realistic t' in exact diagonalization calculations has negligible effect in modifying the results of Ref. 4, plotted in Fig.

1(b). We emphasize that there is a qualitative failure of the single band Hubbard model with fixed U to describe the experimental spectra at higher doping. It is a question of whether the spectra contain two peaks separated by a well defined minimum, or a single peak closer to the Fermi level, Fig. 4(c). The choice of cutoff ω_c used here and in Refs. 4 and 44 provides a quantitative measure of this discrepancy.

ACKNOWLEDGMENTS

We thank P. Phillips for useful comments. This work is supported by the Division of Materials Science and Engineering, U.S. Department of Energy under Contract No. DE-FG02-07ER46352, and benefited from the allocation of supercomputer time at NERSC, Northeastern University's Advanced Scientific Computation Center (ASCC). R.S.M. acknowledges support of a Marie Curie Grant No. PIF-GA-2008-220790 SOQCS.

-
- ¹P. W. Anderson, *Science* **235**, 1196 (1987); **316**, 1705 (2007).
²T. A. Maier, D. Poilblanc, and D. J. Scalapino, *Phys. Rev. Lett.* **100**, 237001 (2008).
³D. J. Scalapino, E. Loh, and J. E. Hirsch, *Phys. Rev. B* **34**, 8190 (1986); **35**, 6694 (1987); J. R. Schrieffer, X. G. Wen, and S. C. Zhang, *ibid.* **39**, 11663 (1989); R. S. Markiewicz and A. Bansil, *ibid.* **78**, 134513 (2008).
⁴H. Eskes, M. B. J. Meinders, and G. A. Sawatzky, *Phys. Rev. Lett.* **67**, 1035 (1991).
⁵A. B. Harris and R. V. Lange, *Phys. Rev.* **157**, 295 (1967).
⁶For a recent review, see P. Phillips, *Rev. Mod. Phys.* **82**, 1719 (2010).
⁷T. Das, R. S. Markiewicz, and A. Bansil, *Phys. Rev. Lett.* **98**, 197004 (2007).
⁸T. Das, R. S. Markiewicz, and A. Bansil, *Phys. Rev. B* **77**, 134516 (2008).
⁹Similar effects are found for charge-transfer insulators (Ref. 4).
¹⁰M. Jarrell, Th. Maier, M. H. Hettler, and A. N. Tahvildarzadeh, *Europhys. Lett.* **56**, 563 (2001).
¹¹T. A. Maier, M. Jarrell, and D. J. Scalapino, *Phys. Rev. B* **74**, 094513 (2006).
¹²E. Pellegrin, N. Nucker, J. Fink, S. L. Molodtsov, A. Gutierrez, E. Navas, O. Strebe, Z. Hu, M. Domke, G. Kaind, S. Uchida, Y. Nakamura, J. Markl, M. Klauda, G. Saemann-Ischenko, A. Krol, J. L. Peng, Z. Y. Li, and R. L. Greene, *Phys. Rev. B* **47**, 3354 (1993).
¹³N. P. Armitage, D. H. Lu, C. Kim, A. Damascelli, K. M. Shen, F. Ronning, D. L. Feng, H. Eisaki, Z.-X. Shen, P. K. Mang, N. Kaneko, M. Greven, Y. Onose, Y. Taguchi, and Y. Tokura, *Phys. Rev. Lett.* **88**, 257001 (2002).
¹⁴Y. Onose, Y. Taguchi, K. Ishizaka, and Y. Tokura, *Phys. Rev. Lett.* **87**, 217001 (2001).
¹⁵Y. Onose, Y. Taguchi, K. Ishizaka, and Y. Tokura, *Phys. Rev. B* **69**, 024504 (2004).
¹⁶S. Uchida, T. Ido, H. Takagi, T. Arima, Y. Tokura, and S. Tajima, *Phys. Rev. B* **43**, 7942 (1991).
¹⁷D. C. Peets, D. G. Hawthorn, K. M. Shen, Y.-J. Kim, D. S. Ellis, H. Zhang, S. Komiya, Y. Ando, G. A. Sawatzky, R. Liang, D. A. Bonn, and W. N. Hardy, *Phys. Rev. Lett.* **103**, 087402 (2009).
¹⁸T. Das, R. S. Markiewicz, and A. Bansil, *Phys. Rev. B* **81**, 174504 (2010).
¹⁹R. S. Markiewicz, S. Sahrakorpi, and A. Bansil, *Phys. Rev. B* **76**, 174514 (2007).
²⁰S. Basak, T. Das, H. Lin, J. Nieminen, M. Lindroos, R. S. Markiewicz, and A. Bansil, *Phys. Rev. B* **80**, 214520 (2009).
²¹S. Sahrakorpi, M. Lindroos, R. S. Markiewicz, and A. Bansil, *Phys. Rev. Lett.* **95**, 157601 (2005); A. Bansil, M. Lindroos, S. Sahrakorpi, and R. S. Markiewicz, *Phys. Rev. B* **71**, 012503 (2005).
²²R. S. Markiewicz and A. Bansil, *Phys. Rev. Lett.* **96**, 107005 (2006).
²³Y. W. Li, D. Qian, L. Wray, D. Hsieh, Y. Xia, Y. Kaga, T. Sasagawa, H. Takagi, R. S. Markiewicz, A. Bansil, H. Eisaki, S. Uchida, and M. Z. Hasan, *Phys. Rev. B* **78**, 073104 (2008).
²⁴Y. Tanaka, Y. Sakurai, A. T. Stewart, N. Shiotani, P. E. Mijnders, S. Kaprzyk, and A. Bansil, *Phys. Rev. B* **63**, 045120 (2001); S. Huotari, K. Hamalainen, S. Manninen, S. Kaprzyk, A. Bansil, W. Caliebe, T. Buslaps, V. Honkimaki, and P. Suortti, *ibid.* **62**, 7956 (2000).
²⁵L. C. Smedskjaer, A. Bansil, U. Welp, Y. Fang, and K. G. Bailey, *J. Phys. Chem. Solids* **52**, 1541 (1991); P. E. Mijnders, A. C. Kruseman, A. van Veen, H. Schut, and A. Bansil, *J. Phys.: Condens. Matter* **10**, 10383 (1998).
²⁶J. Nieminen, H. Lin, R. S. Markiewicz, and A. Bansil, *Phys. Rev. Lett.* **102**, 037001 (2009); J. Nieminen, I. Suominen, R. S. Markiewicz, H. Lin, and A. Bansil, *Phys. Rev. B* **80**, 134509 (2009).
²⁷W. Meevasana, X. J. Zhou, S. Sahrakorpi, W. S. Lee, W. L. Yang, K. Tanaka, N. Mannella, T. Yoshida, D. H. Lu, Y. L. Chen, R. H. He, H. Lin, S. Komiya, Y. Ando, F. Zhou, W. X. Ti, J. W. Xiong, Z. X. Zhao, T. Sasagawa, T. Kakeshita, K. Fujita, S. Uchida, H. Eisaki, A. Fujimori, Z. Hussain, R. S. Markiewicz, A. Bansil, N. Nagaosa, J. Zaanen, T. P. Devereaux, and Z.-X. Shen, *Phys. Rev. B* **75**, 174506 (2007).

- ²⁸In a three-band calculation of the optical spectra, Comanac *et al.* (Ref. 29) found a significant contribution at higher energies from the nonbonding band.
- ²⁹A. Comanac, L. de' Medici, M. Capone, and A. J. Millis, *Nat. Phys.* **4**, 287 (2008); L. de' Medici, X. Wang, M. Capone, and A. J. Millis, *Phys. Rev. B* **80**, 054501 (2009).
- ³⁰It has recently been shown that the high-energy XAS background is associated with the apical oxygen. See T. Ahmed, T. Das, J. J. Kas, H. Lin, B. Barbiellini, F. D. Vila, R. S. Markiewicz, A. Bansil, and J. J. Rehr (unpublished).
- ³¹T. Das, R. S. Markiewicz, and A. Bansil, *Phys. Rev. B* **81**, 184515 (2010).
- ³²C. Kusko, R. S. Markiewicz, M. Lindroos, and A. Bansil, *Phys. Rev. B* **66**, 140513(R) (2002).
- ³³T. Das, R. S. Markiewicz, and A. Bansil, *Phys. Rev. B* **74**, 020506 (2006).
- ³⁴Doping-independent tight-binding parameters have been employed within a rigid band picture. A more realistic treatment of doping effects on electronic states (see, e.g., Refs. 35–37) was not undertaken. However, we expect the rigid band model to be a good approximation for doping away from the Cu-O planes.
- ³⁵A. Bansil, S. Kaprzyk, P. E. Mijnen, and J. Tobola, *Phys. Rev. B* **60**, 13396 (1999); A. Bansil, *Z. Naturforsch., A: Phys. Sci.* **48**, 165 (1993); R. Prasad and A. Bansil, *Phys. Rev. B* **21**, 496 (1980); L. Schwartz and A. Bansil, *ibid.* **10**, 3261 (1974).
- ³⁶S. N. Khanna, A. K. Ibrahim, S. W. McKnight, and A. Bansil, *Solid State Commun.* **55**, 223 (1985); L. Huisman, D. Nicholson, L. Schwartz, and A. Bansil, *Phys. Rev. B* **24**, 1824 (1981).
- ³⁷H. Lin, S. Sahrakorpi, R. S. Markiewicz, and A. Bansil, *Phys. Rev. Lett.* **96**, 097001 (2006).
- ³⁸Phonons may be involved indirectly: (a) if the competing order is a charge-density wave, it may be accompanied by a phonon softening, even though the main effect is electronic [R. S. Markiewicz, J. Lorenzana, G. Seibold, and A. Bansil, *Phys. Rev. B* **81**, 014509 (2010)]; or (b) multiphonon scattering contributes to the broadening of the optical and ARPES Mott feature [A. S. Mishchenko and N. Nagaosa, *Phys. Rev. Lett.* **93**, 036402 (2004); O. Rösch, O. Gunnarsson, X. J. Zhou, T. Yoshida, T. Sasagawa, A. Fujimori, Z. Hussain, Z.-X. Shen, and S. Uchida, *ibid.* **95**, 227002 (2005)].
- ³⁹A different choice for ω_c [P. Phillips and M. Jarrell, *Phys. Rev. Lett.* **105**, 199701 (2010)] was criticized by D. Peets, D. Hawthorn, K. Shen, G. Sawatzky, R. Liang, D. A. Bonn, and W. Hardy, *Phys. Rev. Lett.* **105**, 199702 (2010)].
- ⁴⁰This is also consistent with the QP-GW model: for a fixed $U = 8t$ the pseudogap collapses at an electron-doping $x \sim 0.43$ in NCCO, compared to 0.19 for the doping-dependent U (Ref. 32).
- ⁴¹X. Wang, L. de' Medici, and A. J. Millis, *Phys. Rev. B* **81**, 094522 (2010).
- ⁴²N. Lin, E. Gull, and A. J. Millis, *Phys. Rev. B* **82**, 045104 (2010), and references therein.
- ⁴³C. Weber, K. Haule, and G. Kotliar, *Nat. Phys.* **6**, 574 (2010).
- ⁴⁴A. Liebsch, *Phys. Rev. B* **81**, 235133 (2010)